JCTC Journal of Chemical Theory and Computation

pubs.acs.org/JCTC Article

Discontinuous Molecular Dynamics Simulations of Biomolecule Interfacial Behavior: Study of Ovispirin-1 Adsorption on a Graphene Surface

Size Zheng,* Md Symon Jahan Sajib, Yong Wei, and Tao Wei*

Cite This: J. Chem. Theory Comput. 2021, 17, 1874−1882 Read Online

ACCESS | Metrics & More | Article Recommendations | Supporting Information

ABSTRACT: Fundamental understanding of biomolecular interfacial behavior, such as protein adsorption at the microscopic scale, is critical to broad applications in biomaterials, nanomedicine, and nanoparticle-based biosensing techniques. The goal of achieving both computational efficiency and accuracy presents a major challenge for simulation studies at both atomistic and molecular scales. In this work, we developed a unique, accurate, high-throughput simulation method which, by integrating discontinuous molecular dynamics (DMD) simulations with the Go-like protein−surface interaction model, not only solves the dynamics efficiently, but also describes precisely the protein intramolecular and intermolecular interactions at the atomistic scale and the protein−surface interactions at the coarse-grained scale. Using our simulation method and in-house developed software, we performed a systematic study of α-helical ovispirin-1 peptide adsorption on a graphene surface, and our study focused on the effect of surface hydrophobic interactions and $\pi-\pi$ stacking on protein adsorption. Our DMD simulations were consistent with full-atom molecular dynamics simulations and showed that a single ovispirin-1 peptide lay down on the flat graphene surface with randomized secondary structure due to strong protein−surface interactions. Peptide aggregates were formed with an internal hydrophobic core driven by strong interactions of hydrophobic residues in the bulk environment. However, upon adsorption, the hydrophobic graphene surface can break the hydrophobic core by denaturing individual peptide structures, leading to disassembling the aggregate structure and further randomizing the ovispirin-1 peptide's secondary structures.

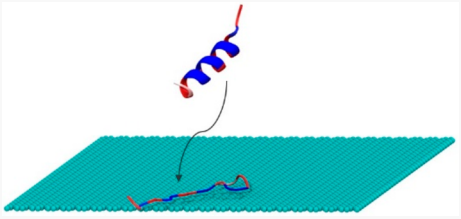

1. INTRODUCTION

Biomolecular interfacial behavior, such as protein adsorption at the solid−solution interface, has been a research focus for more than four decades due to its critical role in the development of biomaterials,[1−3] nanomedicine,[4,5] nanoparticle-based biosensing technologies[6,7] such as surface-enhanced Raman spectrum using gold or silver nanoparticles,[6,7] and in the marine industry.[8] Protein adsorption mediates biofouling, introducing the subsequent attachment of microorganisms and the foreign response.[3,9,10] The attachment of bacteria, fungi, mussels, barnacles, and seaweeds onto ship hulls leads to an increase in the hydrodynamic drag on vessels' sailing movement[11] and causes corrosion of vessels' metal surfaces. To control marine biofouling costs, governments and industries around the world invest billions of dollars annually.[8] Antibiofouling also presents a major challenge for blood-contact biomedical devices, biocompatible materials, and nanomedicine.[12,13] The attached proteins and microorganisms alter the surfaces' chemico-physical properties and consequently change the device's sensitivity or materials' functionality. Fundamental in-depth understanding of protein adsorption at the atomistic and molecular scales is highly desirable despite a significant amount of previous studies.[1−3,9,10,14,15]

The complexity of the protein adsorption process arises from various factors, such as surface charge distribution,[16] morphology,[17,18] roughness,[19,20] wettability,[21] buffer's ions,[10] and the protein surface's heterogeneity[22] in charge and hydrophobicity. The water-mediated hydrophobic, hydration forces, and electrostatic interactions were found to be the most important factors.[14,15] Conventional atomistic molecular dynamics (MD) simulations have been widely used in the study of protein adsorption on different substrate surfaces.[17,20,22−29] Atomistic MD simulations can probe molecular structures with atomistic resolutions and sample the events from subnanoseconds to microseconds.[17,30−32] However, the computational load of atomistic MD simulations for a large-sized system while retaining atomistic details in a long process is prohibitively expensive,[17,33] particularly with the explicit water model. The coarse-grained (CG) MD simulations can achieve significant efficiency by lowering the model's resolution where a number of atoms are grouped as a CG particle and the

Received: November 10, 2020
Published: February 15, 2021

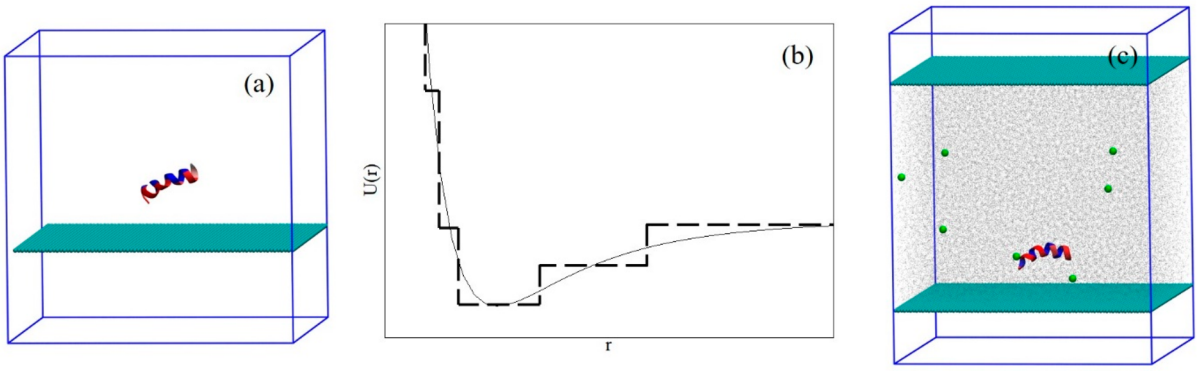

Figure 1. (a) Snapshot of the initial configuration of DMD (10.0 × 10.0 × 10.0 nm^3): graphene (cyan) on the $X-Z$ plane (the Y-axis is normal to the plane), ovispirin-1 peptide (the hydrophobic residues were colored blue and the hydrophilic residues red); (b) diagram of potential profiles for peptide/protein interaction with the surface (the solid curve represents the continuous potential and the dashed lines for the discretized potential); (c) snapshot of the initial configuration of atomistic MD (10.32 × 10.64 × 13.10 nm^3): graphene (cyan) on the $X-Y$ plane (the Z-axis is normal to the plane), ovispirin-1 peptide (the hydrophobic residues are colored blue and the hydrophilic residues are red), water (gray), and Cl^- counterions (green).

intramolecular interaction functions are also simplified.[34] However, CG MD simulation parameterized with the most widely used Martini force field, which imposes an elastic network to connect the CG beads, cannot present protein's secondary structural changes.[35,36]

Discontinuous molecular dynamics (DMD) is an extremely efficient alternative to the conventional atomistic MD using continuous force field, introduced by Alder and Wainwright[37] in 1959 for simulations of hard spheres. It has been widely applied to simulations of polymer chains[38−40] and protein folding and aggregation.[41−49] DMD uses an event-driven MD method and simulates the potentials applied on particles by discontinuous step-functions of interparticle distance. Thus, atoms/particles move at constant velocities until their distance becomes equal to the point of a discontinuity, where the program performs a calculation of the interactions by solving the conservations of momentum and energy simultaneously. In other words, the time step in DMD can be adaptive and much larger than 1−2 fs as applied in the atomistic MD. Previous research[50] has demonstrated that a DMD simulation can be up to 100 times more efficient than an atomistic MD simulation in implicit water. Therefore, the trajectory and potential of a particle can be simulated discontinuously and at a long-time scale. Both coarse-grained[41−49] and atomistic models[51−53] have been adopted in DMD to study a complex biological system at large time and spatial scales, which are difficult for atomistic MD simulations to handle. We used DMD to successfully simulate the aggregation of polyalanines, the configuration of which is intended to mimic the hydrophobic part of β-amyloid, under bulk conditions[54] and in a confined medium,[55] and the aggregation of dipeptide repeat proteins[56,57] which are associated with amyotrophic lateral sclerosis and frontotemporal dementia. Those simulations,[54−57] which covered the whole dynamic process from ab initio to the final equilibrium state, cost shorter computational time compared with the conventional atomistic MD, and matched experimental measurements.

On the basis of the previous works on protein folding,[58−60] an efficient coarse-grained Go-like model[61] in implicit water was recently further developed to study protein−surface interactions. It was successfully employed to predict the orientation of peptide/protein on polymer and graphene surfaces in comparison to the experimental measurement using sum frequency generation (SFG) vibrational spectroscopy.[62−65]

To achieve sufficient computational efficiency without compromising accuracy and to present protein's secondary structural changes, we integrated the Go-like model[61] into our in-house developed framework of DMD simulations.[66] The original DMD full-atom force field[51] was utilized to compute the intermolecular and intramolecular interactions of proteins precisely and efficiently at the atomistic level. The coarse-grained Go-like model was employed to calculate the peptide/protein interactions with the surface at the CG level. To study the effect of the substrate surface's hydrophobicity and $\pi-\pi$ stacking on protein adsorption while excluding the influence of other factors, we chose a model system of a flat graphene surface and a small-sized antibiotic ovispirin-1 peptide which consists of 18 amino acid residues with approximately 78% helix structure. Our results of the DMD simulation in implicit water were further verified with conventional atomsitic MD simulations in explicit water. Our unique method combining the merits of both the DMD simulations and the Go-like model will also be crucial to high-throughput studies of peptide/protein interactions with surfaces. Our fundamental study of peptide/protein adsorption will pave the way for future development of biomaterials and biosensing techniques. The rest of this article is organized as follows: section 2 provides the details of the implementation of DMD simulations and atomistic MD simulations; section 3 discusses the simulation results; and the article then concludes with a summary in section 4.

2. METHOD

2.1. DMD Simulations. To study protein/peptide adsorption, we modified our in-house developed DMD simulation software, which was published with the source code in our previous paper,[66] by incorporating the CG Go-like model[61] for biomolecule−surface interactions. It is noteworthy that due to the event-driven nature of DMD and the implicitly represented solvent, it is not straightforward to correlate simulation time and temperature with real physical time and temperature.[52,67−69] Thus, we used time step t^*, and reduced temperature $T^* = T/T_s$, instead of the real units, to represent

https://dx.doi.org/10.1021/acs.jctc.0c01172
J. Chem. Theory Comput. 2021, 17, 1874−1882

Table 1. χ Values of Different Residues and Surfaces[a]

residue name	GLY	ALA	PRO	VAL	LEU	ILE	MET	PHE	TYR	TRP	SER	CYS
χ	−0.4	1.8	−1.6	4.2	3.8	4.5	1.9	2.8	−1.3	−0.9	−0.8	2.5
residue name	ASN	GLN	LYS	HIS	ARG	ASP	GLU	THR	PHO	PHI	RPH	
χ	−3.5	−3.5	−3.9	−3.2	−4.5	−3.5	−3.5	−0.7	4.5	−1.0	1.5	

[a]Hydrophobic residues/surfaces have more positive values while hydrophilic residues/surfaces have more negative values. "PHO" is the hydrophobic surfaces; "PHI" represents the hydrophilic surfaces; and "RPH" is the relative-hydrophobic surfaces.

the time scale and temperature in the simulation. To determine T_s, we set $\mathcal{N}k_BT_s = E$, where $\mathcal{N}$ stands for Avogadro's number, k_B for Boltzmann's constant, and E for one unit of energy, taken to be 1 kcal/mol. We thus obtained T_s = 503.2 K and set T^* = 0.57. The real temperature, therefore, is 286.82 K, which is close to 300 K in the atomistic MD simulation. As will be discussed later, our DMD bulk simulations at such a temperature show no denaturing of the ovispirin-1 peptide, which is in agreement with the atomistic MD simulation with explicit water.

Solvation simulations were first carried out in the bulk environment without the presence of a graphene surface, and then adsorption simulations were performed with the peptide(s) placed around 2.0 nm away from the implicit surface, both of which were inside a box with the dimensions of 10 × 10 × 10 nm^3 (Figure 1a), with periodic boundary conditions (PBC) in all X, Y, and Z directions. The simulations were started with energy minimization, followed by a series of short-runs that gradually increased the temperature from 0.4 to 0.57. At each temperature step, the system was relaxed for 2 × 10^4 timesteps, following the protocol published in our previous studies.[54−57] Then the production runs were carried out at the temperature of 0.57 in the NVT ensemble until the time step reached 2 × 10^6. Each simulation took about 36 h to finish by serial computation on an AMD Ryzen 9 3900X clocked at 3.8 GHz. In addition, we performed simulations of multiple-peptide adsorption by using the dimensions of the system box and procedures aforementioned.

As stated in Section 1, the intra- and intermolecular interactions of peptide(s) in the aqueous environment were represented by an all-atom molecular model in implicit water with force field parameters for DMD simulations from the literature.[51] The interactions between peptide/protein residues and substrate surface, however, were represented by the Go-like model,[61,70] which can present the main graphene's surface effects on protein adsorption: surface hydrophobicity interactions and $\pi-\pi$ stacking. The potential function is as follows:

$$V_{\text{surface}} = \sum_{i}^{N} \left\{ \pi\rho\sigma_i^3\epsilon_i \left[\theta_1 \left(\frac{\sigma_i}{z_{is}}\right)^9 - \theta_2 \left(\frac{\sigma_i}{z_{is}}\right)^7 + \theta_3 \left(\frac{\sigma_i}{z_{is}}\right)^3 - (\theta\chi_s + \theta_p(\chi_{pi} + 2\delta)) \left(\frac{\sigma_i}{z_{is}}\right)^3 \right] \right\}$$

where N stands for the residues' number in a peptide/protein, z_{is} for the distance between residue i and the surface, and σ_i and ϵ_i for the van der Waals parameters. The first three terms ($\left(\frac{\sigma_i}{z_{is}}\right)^x$, x = 9, 7, and 3) in the above equation are to calculate the interactions of a surface with amino acid residue of any type, while the fourth term describes the differences of residues and surfaces in terms of hydrophobicity χ, and the side chain planarity. Thus, the interaction of peptide/protein with the surface is controlled by the surface hydrophobicity and side chain planarity, which can lead to side chain-surface $\pi-\pi$ interactions. In the Go-model potential equation, the parameters θ_s and χ_s of the fourth term control the hydrophobicity of the surface, while the parameters θ_p and χ_p control the hydrophobicity of each amino acid in the peptide/protein, and δ controls the side chain's planarity. The hydropathy indices of all 20 types of amino acids and 3 types of surfaces are listed in Table 1. The graphene surface was simulated as a relative-hydrophobic (RPH) surface with χ = 1.5, as in the previous studies.[64,70] The values of the other parameters used in the equation can be found in Table S1 in the Supporting Information.

In DMD, the original continuous potential profile of peptide/protein interactions with the surface was discretized and represented by step functions (Figure 1b for an example). During discretization, the cutoff distance is set at 10.0 Å and the minimum distance is at where the potential reaches positive 1.0 kcal/mol. The jump number of the step function is adaptive based on the potential profile: once the distance gap between two adjacent jumps reaches 2 Å, or the distance gap between one jump and the position of the lowest potential reaches 1 Å, we will add a step in the function. The values of discretized potentials for the interactions of different amino acid residues with the graphene surface are listed in Table S2. Detailed information on the discretization of protein−protein interactions in DMD simulations was reported in our previous paper.[66]

In the Go-like model, each amino acid residue was simplified as a CG bead with its center of mass located on the α-carbon of the residue in the all-atom model. Thus, in mapping the CG model to the all-atom model, the surface's force acting on each CG bead was assigned to the α-carbon of an amino acid residue and then dissipated by the interactions of the α-carbon atom with its surrounding atoms. The whole process is energy and momentum conserved. The ovispirin-1 peptide's solution structure in both DMD and atomistic MD simulations was obtained from the protein data bank (pdb code: 1HU5).

2.2. Atomistic MD Simulations. Atomistic MD simulations were carried out using the GROMACS package[71] (version 4.6.5), TIP4P water model, and OPLS-AA force field,[72,73] which can present the graphene surface hydrophobic interactions and $\pi-\pi$ stacking precisely and was widely used for many previous studies of graphene/water[74] and graphene/water/protein interactions.[26,75−77] The details about the parameters of graphene atoms' intermolecular and intramolecular interactions are illustrated in the Supporting Information (Table S3). PBC conditions were applied to the system along the X, Y, and Z directions. To mimic an infinitely large graphene surface without boundary effects on adsorption, graphene surface atoms were bonded with PBC atoms and the positions of three surface atoms at the edges were fixed, which allows certain surface fluctuations.

https://dx.doi.org/10.1021/acs.jctc.0c01172
J. Chem. Theory Comput. 2021, 17, 1874−1882

The dynamic equations were integrated by using the leapfrog algorithm with a time step of 1 fs. The ovispirin-1 peptide was initially placed far away from a graphene surface (~1 nm) with negligible surface−peptide interactions, as shown in Figure 1c. Another graphene sheet was placed on the top as a restraining layer to keep all molecules inside the simulation box while allowing a peptide to interact with either graphene layer. The space between two graphene sheets was filled with water molecules with a thickness of 9.1 nm, which is large enough to decouple interactions from the top and bottom surfaces. In addition, there are two vacuum slabs of 2.0 nm thickness, one at the bottom and one at the top of the cell, to remove the interactions between the atoms inside the cell and their images along the *Z*-direction and thus save computation. The total size of the simulation system is 10.32 × 10.64 × 13.10 nm^3.

The MD simulations were started with the relaxation of water molecules with a short-run at 300 K, keeping all peptide atoms' positions fixed. Then the production runs were carried out in the NVT ensemble at 300 K for 85 ns without any constraint of the peptide atoms. The system temperature was maintained with a Nosé-Hoover thermostat. The Particle Mesh Ewald summation was utilized to calculate the long-range electrostatic interactions, with a cutoff distance of 1.2 nm for the separation of the direct and reciprocal space. A spherical cutoff at 1.2 nm was imposed on the LJ interactions. The long-range dispersion effect on energy and pressure was also incorporated.

3. RESULTS AND DISCUSSION

3.1. Simulations of Single-Peptide Adsorption. We first performed the bulk simulation of ovispirin-1 peptide without the graphene surfaces using a DMD simulation in an implicit water environment to compare with a conventional atomistic MD simulation using explicit water. Consistent with the atomistic MD simulation, an ovispirin-1 peptide remained stable in its secondary structure in the DMD simulation (see the snapshot of Figure S1). Our results also matched the solution NMR measurement published in the literature,[78] which showed that ovispirin-1 retained a helical structure in the solution. This also demonstrates that DMD simulations with atomistic resolution in the implicit water environment can precisely present the ovispirin-1 folding.

Subsequently, five independent runs of adsorption simulations on the graphene surface were performed using various initial configurations to validate the consistency using DMD simulation with the Go-like model for protien-surface interactions. To demonstrate the adsorption process, we monitored one adsorption trajectory (see snapshots in Figure 2) and the secondary structure evolution upon adsorption (Figure 3). At time step $t = 8 \times 10^4$, the ovispirin-1 peptide was about 2.4 nm above the graphene surface (Figure 2a). Since the peptide was allowed to diffuse freely in the system, at $t = 5.174 \times 10^5$, it landed on the surface at the site near its N-terminal, where there was a hydrophobic amino acid residue of LEU3 (Figure 2b). Subsequently, the peptide was quickly adsorbed onto the surface at $t = 5.311 \times 10^5$ (Figure 2c). At the initial landing on the graphene surface, the peptide underwent fluctuations in the secondary structure (Figure 3). Then the peptide rolled on the surface to allow the hydrophobic residues to contact the graphene surface. Up to this point, the peptide still preserved its original helical secondary structure (Figure 3). Shortly after the peptide lay down on the surface, its N-terminal started to denature first. The denaturation then gradually propagated toward the C-terminal (Figure 3). Eventually, at $t = 2 \times 10^6$ (Figure 2d), the whole peptide's structure completely denatured to random coil and small content of turn structure (Figure 3). It is notable that the peptide's structure could be altered upon landing, as shown in Figures S2 and S3.

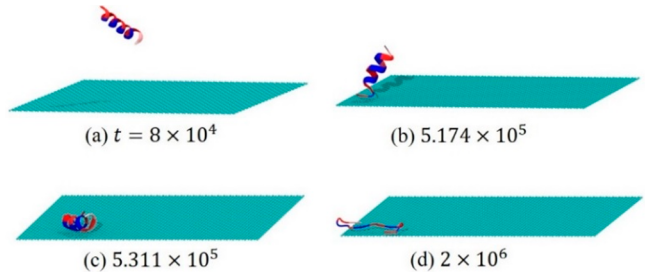

Figure 2. Snapshots of the adsorption process of an ovispirin-1 peptide on the graphene surface: (a) the peptide was more than 2 nm above the graphene surface; (b) the peptide diffused toward the surface and its N terminal landed on the surface; (c) the peptide fell down and its hydrophobic residues came into contact with the surface; (d) the peptide's structure denatured eventually and became a random coil. The hydrophobic residues are colored blue, and the hydrophilic ones are red.

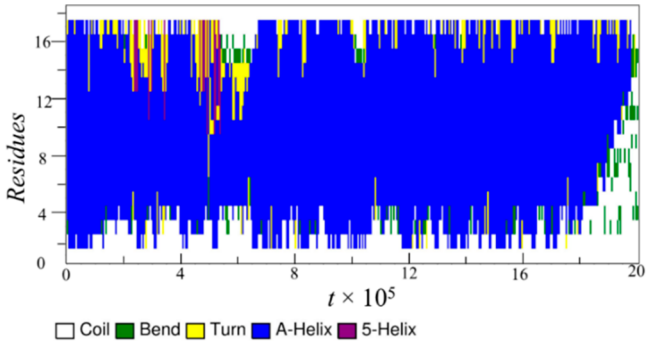

Figure 3. Secondary structure evolution upon ovipirin-1 adsorption. The DSSP algorithm was used to deconvolute the secondary structure of ovispirin-1 peptide.

Figure 4a shows that for the five independent simulations, the distances of all the residues of ovispirin-1 peptide to the graphene surface were different and more than 2.0 nm away from the surface except in the second case. However, at the end of the simulations, all those residues moved to the surface with very similar residue-surface gapping distance (Figure 4b) and the peptides in all cases lay on the surface, indicating that the final results of ovispirin-1 peptide adsorption were independent of the peptide's initial position and orientation above the surface. This also demonstrated the consistency of the simulation results of DMD. Figure 4 shows that the hydrophobic residues, including LEU3, ILE6, ILE10, ILE11, ILE13, ILE14, and GLY18, had smaller distances to the surface compared to the neutral and hydrophilic residues. This also suggests that hydrophobic interactions of the peptide-surface served as the key driving force for ovispirin-1 adsorption on the hydrophobic graphene surface. The observations of DMD in this work are consistent with the findings of our previous studies of single-peptide adsorption, using large-scale CGMD simulations,[35] atomistic MD simulation, and free energy computation.[26] Our previous studies[26] showed that both

https://dx.doi.org/10.1021/acs.jctc.0c01172
J. Chem. Theory Comput. 2021, 17, 1874−1882

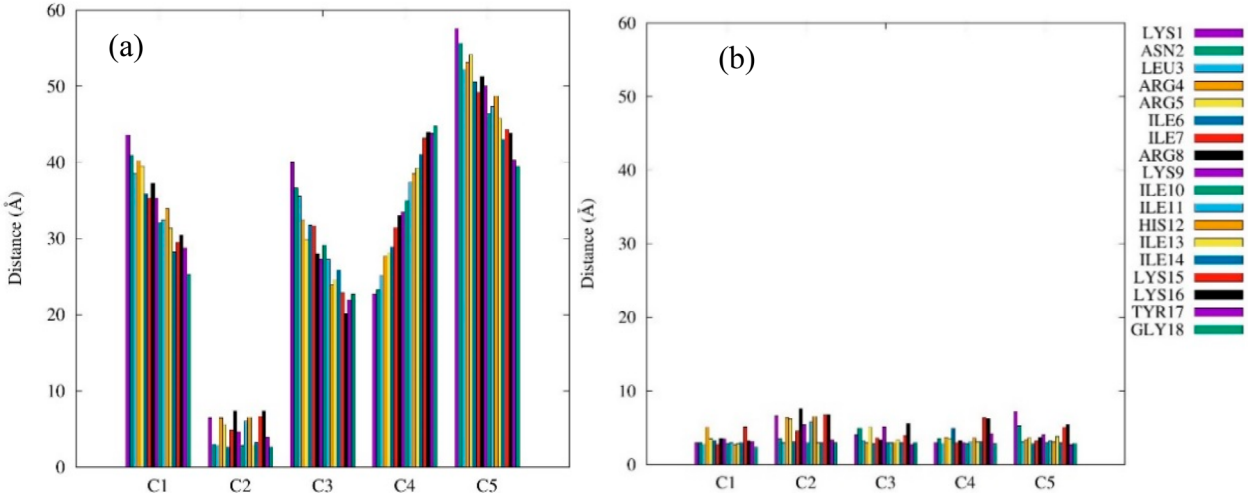

Figure 4. Distance of each residue of ovispirin-1 to the graphene surface from five independent simulations (a) in the initial state, and (b) in the final equilibrium state.

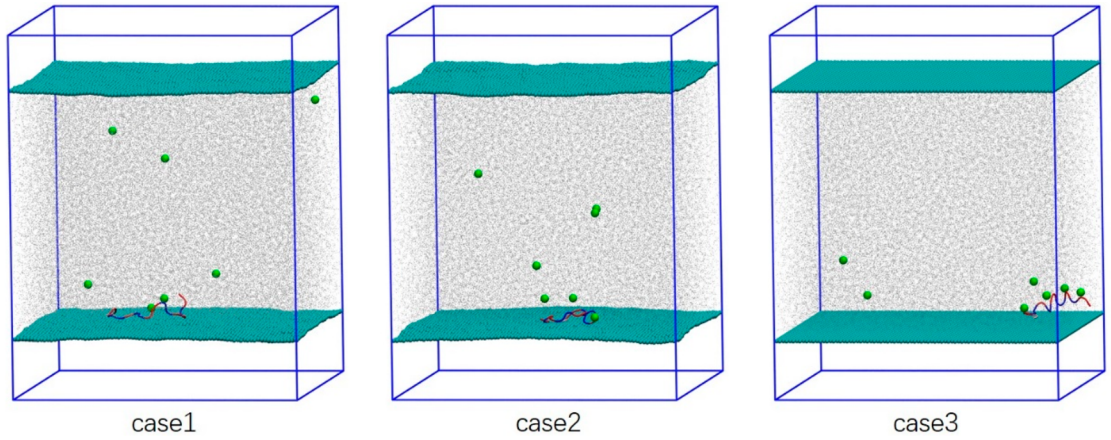

Figure 5. Snapshots of the final states of ovispirin-1 adsorption on the graphene surface with explicit water in three different cases of atomistic MD simulations. The hydrophobic residues are colored blue, and the hydrophilic ones are red.

protein−surface interactions and the surface-solvent short-range hydrophobicity effect, that is, $\gamma \cdot \Delta A$ (γ, the surface tension; ΔA, the available surface contact area), were driving forces for protein adsorption on a neutral hydrophobic surface. A protein is more likely to lie down on a hydrophobic surface with a larger ΔA to achieve minimum free energy.[26] As elucidated in the Method section, in our DMD simulations, the effect of surface hydration/dehydration was implicitly incorporated in the peptide-surface interactions. The lying-down peptide can achieve larger peptide-surface attraction compared to other orientations.[26] Similar to our observation in this work, our previous simulations[35] of hybrid CGMD and atomistic MD showed that the helical structure of ovispirin-1 peptide was completely randomized on the hydrophobic gold surface.

In all these five simulations, the ovispirin-1 peptide landed on the graphene surface with its terminals, though the landing site can be either the N-terminal or the C-terminal. To further investigate the initial landing site, we performed 15 additional simulations with three typical initial orientations: the N-terminal toward the surface, the C-terminal toward the surface, and the axis of the ovispirin-1 parallel to the surface. For each of the three different initial orientations, five independent simulations were performed using different initial velocity profiles. Our simulations showed that the ovispirin-1 had higher possibilities of landing with its N-terminal than the C-terminal. However, if the ovispirin-1 was initially parallel to the surface, the landing site showed no specific preference of the orientation. This suggests that the landing site of ovispirin-1 on the graphene surface was not specific, although eventually in all cases the peptide would lie down on the graphene surface. An ovispirin-1 peptide can adopt various landing sites due to the complexity of the adsorption free energy profile, where multiple sites with local free energy minimum are present.[24]

To further validate the DMD simulations, we performed three atomistic MD simulations in explicit water using different initial configurations and initial velocity profiles. Their final configurations were shown in Figure 5. Consistent with the DMD simulations, all atomistic MD simulations showed that the peptides lay down on the graphene surface and completely denatured to random coils, which validated the accuracy of our method of DMD simulations with the Go-like model. It should also be emphasized that it only took ∼36 core-hours of computation with DMD to simulate the whole process, whereas it took ∼2880 core-hours with conventional atomistic MD.

It is notable that our DMD simulations were performed at the atomistic and coarse-grained levels to illustrate the main effects of the graphene surface: surface hydrophobic inter-

https://dx.doi.org/10.1021/acs.jctc.0c01172
J. Chem. Theory Comput. 2021, 17, 1874−1882

actions and $\pi-\pi$ stacking. The factor of hydration and dehydration was also implicitly included in the Go-like model that we adopted. The Go-like model for the specific graphene surface was validated with many experimental results (protein adsorption and orientation) in previous publications.[64,79] Under the surface's influence, the ovispirin-1 peptide(s) was found to be adsorbed onto the surface with randomized secondary structure. The residue of tyrosine (TYS17) was found to lie on the surface due to the $\pi-\pi$ stacking of the residue's aromatic group and the graphene surface in both DMD and atomistic MD simulations. We used the parameters of DMD for protein folding and the Go-like model for protein−surface interactions, which have been calibrated with atomistic MD simulations and experimental data.[61,80] Moreover, the Go-like model as presented in the previous papers[61] was calibrated with the potential of mean force, which includes the overall effect of the surface, amino acid residues, and solvent. Our DMD simulation code was also used to present protein folding in the bulk environment in several of our previous papers.[56,57,66] In this work, our simulations of ovispirin-1 peptide adsorption are in agreement with atomistic MD simulations. Moreover, we compared the simulated secondary structure of the peptide in the bulk environment with the solution structure (pdb code 1HWA) measured with an NMR experiment,[81] which further validated our DMD simulations (see Figure S1).

3.2. Simulations of Peptide Aggregate Adsorption. We also simulated the adsorption behavior of multiple peptides on a graphene surface. As a reference, we first performed the DMD simulations of four ovispirin-1 peptides in the bulk environment (the concentration of 14.02 g/L) without a graphene surface. The four peptides were randomly distributed initially in the simulation box; however, they eventually formed a rounded tetramer with a hydrophobic core, with the hydrophilic residues exposed outwardly to the bulk (Figure 6). The hydrophobic amino residues (LEU3, ILE6-7, ILE10-11 and ILE13-14) of the ovispirin-1 peptides merged to stabilize the core structure of the aggregates. This is similar to the aggregate structure reported in our previous study[82] of the aggregation of polyalanines.

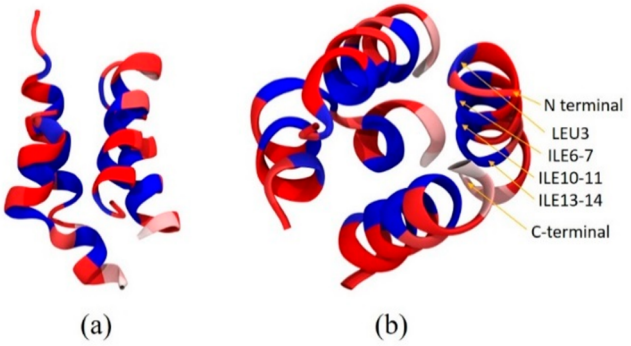

Figure 6. Tetramer formed by four ovispirin-1 peptides in the bulk simulated by DMD with the Go-like model: (a) front view, (b) top view. The hydrophobic residues came into contact with each other to form a hydrophobic core. The hydrophobic residues, including LEU3, ILE6-7, ILE10-11, and ILE13-14, are colored blue, and the hydrophilic ones are red.

Next, the adsorption of peptide aggregate on the graphene surface was simulated by using the equilibrated tetramer in the bulk environment as the initial conformation. As shown in Figure 7a, the tetramer was initially placed about 2 nm away from the graphene surface. After 1.1×10^6 timesteps, the tetramer was adsorbed on the surface with the secondary structure preserved (Figure 7b). However, under the hydrophobic effect of the graphene surface, the tetramer disassembled and the individual peptides were separated from each other (Figure 7c). Each individual peptide underwent structural alternation, and the helical structure was randomized eventually (Figure 7d).

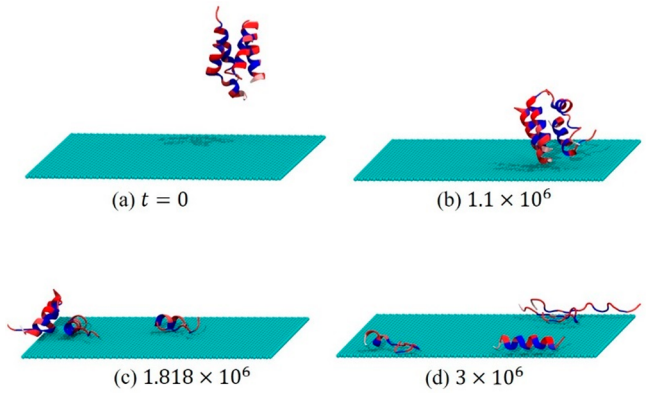

Figure 7. Snapshots of the adsorption process of the ovispirin-1 tetramer on the graphene surface: (a) tetramer was initially about 2 nm away from the graphene surface; (b) tetramer landed on the surface, keeping its original secondary structure; (c) tetramer disassembled and the individual peptides were separated apart; (d) three of the four individual peptide denatured eventually and became random coils. The hydrophobic residues are colored blue, and the hydrophilic ones are red.

Looking at the disassembling process in detail, we can find that it started with the denaturing of one individual peptide, which had its terminal in contact with the graphene surface and led to the breaking of the hydrophobic core. The standing peptides fell down on the graphene, separated from the tetramer and denatured ultimately (Figure 8).

It should be noted that as shown in previous DMD simulation papers,[52,67,68] it is not straightforward to correlate the simulation time of DMD with real physical time due to its event-driven nature and the implicit solvent used. Marchut and

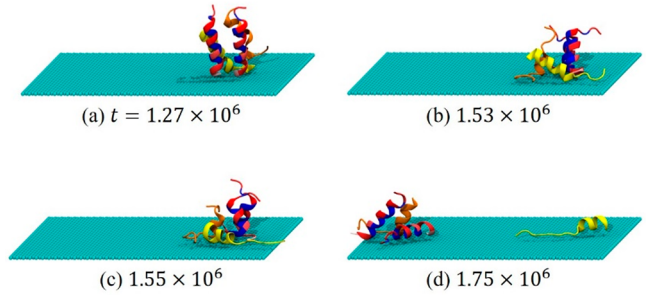

Figure 8. Snapshots of the ovispirin-1 tetramer disassembling process during the simulation corresponding to Figure 7. (a) The tetramer landed on the graphene surface vertically; (b) one of the peptide (orange) denatured first and broke the hydrophobic core; (c) the neighboring peptide (yellow) fell down on the surface and started to denature; (d) The yellow peptide diffused away from the tetramer while the aggregate disassembling continued.

https://dx.doi.org/10.1021/acs.jctc.0c01172
J. Chem. Theory Comput. 2021, 17, 1874−1882

Hall[68] proposed to estimate the time scale in three different ways: (1) The first estimate was based on the fact that approximately 90% of the simulation events in DMD were bond events. If one assumes that two bond events are equivalent to a bond vibration, and that each bond vibration happens as quickly as a carbon−carbon single bond vibration (0.02 ps), the time covered in 1 billion collisions would be roughly 10 μs. (2) The second estimate was based on the fact that α helices fold in roughly 100 ns,[83] and that the α helices in their model folded in 250 million collisions. Thus, the time covered in 1 billion collisions would be about 0.4 μs. (3) The third estimate was based on the fact that β sheets fold in roughly 1 ms,[83] and their results demonstrated β sheets forming in 8 billion collisions. In this case, the time covered in 1 billion collisions would be roughly 125 μs. In our simulations, the numbers of bond and collision events are about 5 billion and 1.25 billion, respectively, which means that the converted time scales would be about 50 μs (based on estimate 1), 0.5 μs (based on estimate 2), and 156.25 μs (based on estimate 3).

4. CONCLUSION

Despite extensive studies of protein adsorption,[10,17,20,27,62−65,84,85] a high throughput simulation methodology with sufficient computational efficiency and accuracy at the atomistic and molecular scales is highly desired to rationalize experimental design and synthesis for various applications, such as antibiofouling materials, and nanoparticle-based sensing technology. Moreover, simulations involving biomolecules of sophisticated structures require high resolution at the atomistic scale. The main challenging issue for atomistic MD simulations of a protein−surface in an aqueous environment is the significant computational load, particularly with the large amount of explicit water molecules. In this work, we developed a novel simulation method based on the DMD simulation framework and incorporate the Go-like protein−surface interaction model. The event-driven DMD simulations provide the capability of solving the dynamics efficiently. Furthermore, the protein's intramolecular and intermolecular interactions, and protein−surface interactions, can be precisely described in the implicit water environment using the original full-atom DMD simulation parameters and the Go-like model, respectively.

We utilized our hybrid simulation method and in-house developed code to study the interactions of an ovispirin-1 peptide with a graphene surface. Our simulation system focused on the effects of surface's hydrophobicity and $\pi-\pi$ stacking on protein adsorption without involving other complex factors of the substrate surface, that is, morphology and charges. Our simulations demonstrated that a single ovispirin-1 peptide was prone to lying down on the graphene surface with the denatured secondary structure upon adsorption due to the surface's hydrophobic interactions and graphene−amino acid residues' $\pi-\pi$ stacking. Our DMD simulation results of ovispirin-1 peptide adsorption (orientations and structures) were further validated using the conventional atomistic MD simulations in explicit water. Our simulations also showed that the ovispirin-1 peptides can form stable aggregates with an inner hydrophobic core driven by the strong interactions of the hydrophobic residues among different peptide molecules. Upon adsorption, the hydrophobic surface randomized the individual peptide's structure and introduced the disassembling of the aggregate and further denaturing of the peptides' secondary structures. This fundamental study of peptide/protein adsorption will be crucial to future broad applications.

■ ASSOCIATED CONTENT

Supporting Information

The Supporting Information is available free of charge at https://pubs.acs.org/doi/10.1021/acs.jctc.0c01172.

Values of the other parameters used in the equation of $V_{surface}$; discretized potentials (kcal/mol) as a function of the distance (Å) of amino acid residues to the surface; parameters used to model graphene in aaMD simulation; additional figures that support the text (PDF)

■ AUTHOR INFORMATION

Corresponding Authors

Size Zheng − *College of Materials and Chemistry & Chemical Engineering, Chengdu University of Technology, Chengdu, Sichuan 610059, P. R. China;* orcid.org/0000-0001-5719-1918; Email: zhengsize19@cdut.edu.cn

Tao Wei − *Chemical Engineering Department, Howard University, Washington, D.C. 20059, United States;* orcid.org/0000-0001-6888-1658; Email: tao.wei@howard.edu

Authors

Md Symon Jahan Sajib − *Chemical Engineering Department, Howard University, Washington, D.C. 20059, United States*

Yong Wei − *Department of Computer Science and Information Systems, University of North Georgia, Dahlonega, Georgia 30597, United States*

Complete contact information is available at: https://pubs.acs.org/10.1021/acs.jctc.0c01172

Notes

The authors declare no competing financial interest.

■ ACKNOWLEDGMENTS

T. Wei acknowledges the grant support from the National Science Foundation (NSF 1943999). T. Wei is grateful for the computational resources from the program of Extreme Science and Engineering Discovery Environment (XSEDE) and the Texas Advanced Computing Center (TACC).

■ REFERENCES

(1) Leonardi, A. K.; Ober, C. K. Polymer-based marine antifouling and fouling release surfaces: strategies for synthesis and modification. *Annu. Rev. Chem. Biomol. Eng.* **2019**, *10*, 241−264.

(2) Barry, M. E.; Davidson, E. C.; Zhang, C.; Patterson, A. L.; Yu, B.; Leonardi, A. K.; Duzen, N.; Malaviya, K.; Clarke, J. L.; Finlay, J. A.; et al. The role of hydrogen bonding in peptoid-based marine antifouling coatings. *Macromolecules* **2019**, *52* (3), 1287−1295.

(3) Jiang, S.; Cao, Z. Ultralow-fouling, functionalizable, and hydrolyzable zwitterionic materials and their derivatives for biological applications. *Adv. Mater.* **2010**, *22* (9), 920−932.

(4) Ventola, C. L. Progress in nanomedicine: approved and investigational nanodrugs. *Pharm. Ther.* **2017**, *42* (12), 742.

(5) Voskerician, G.; Shive, M. S.; Shawgo, R. S.; Von Recum, H.; Anderson, J. M.; Cima, M. J.; Langer, R. Biocompatibility and biofouling of MEMS drug delivery devices. *Biomaterials* **2003**, *24* (11), 1959−1967.

(6) Yi, M.; Lau, C. H.; Xiong, S.; Wei, W.; Liao, R.; Shen, L.; Lu, A.; Wang, Y. Zwitterion−Ag Complexes That Simultaneously Enhance

Biofouling Resistance and Silver Binding Capability of Thin Film Composite Membranes. *ACS Appl. Mater. Interfaces* **2019**, *11* (17), 15698−15708.
(7) Sun, F.; Hung, H.-C.; Sinclair, A.; Zhang, P.; Bai, T.; Galvan, D. D.; Jain, P.; Li, B.; Jiang, S.; Yu, Q. Hierarchical zwitterionic modification of a SERS substrate enables real-time drug monitoring in blood plasma. *Nat. Commun.* **2016**, *7* (1), 1−9.
(8) Schultz, M.; Bendick, J.; Holm, E.; Hertel, W. Economic impact of biofouling on a naval surface ship. *Biofouling* **2011**, *27* (1), 87−98.
(9) Tsai, W. B.; Grunkemeier, J. M.; Horbett, T. A. Human plasma fibrinogen adsorption and platelet adhesion to polystyrene. *J. Biomed. Mater. Res.* **1999**, *44* (2), 130−139.
(10) Wei, T.; Kaewtathip, S.; Shing, K. Buffer effect on protein adsorption at liquid/solid interface. *J. Phys. Chem. C* **2009**, *113* (6), 2053−2062.
(11) So, C. R.; Yates, E. A.; Estrella, L. A.; Fears, K. P.; Schenck, A. M.; Yip, C. M.; Wahl, K. J. Molecular recognition of structures is key in the polymerization of patterned barnacle adhesive sequences. *ACS Nano* **2019**, *13* (5), 5172−5183.
(12) Damodaran, V. B.; Murthy, N. S. Bio-inspired strategies for designing antifouling biomaterials. *Biomater. Res.* **2016**, *20* (1), 18.
(13) Francolini, I.; Vuotto, C.; Piozzi, A.; Donelli, G. Antifouling and antimicrobial biomaterials: an overview. *Apmis* **2017**, *125* (4), 392−417.
(14) Ostuni, E.; Chapman, R. G.; Holmlin, R. E.; Takayama, S.; Whitesides, G. M. A survey of structure− property relationships of surfaces that resist the adsorption of protein. *Langmuir* **2001**, *17* (18), 5605−5620.
(15) Chapman, R. G.; Ostuni, E.; Takayama, S.; Holmlin, R. E.; Yan, L.; Whitesides, G. M. Surveying for surfaces that resist the adsorption of proteins. *J. Am. Chem. Soc.* **2000**, *122* (34), 8303−8304.
(16) Chen, S. F.; Cao, Z. Q.; Jiang, S. Y. Ultra-low fouling peptide surfaces derived from natural amino acids. *Biomaterials* **2009**, *30* (29), 5892−5896.
(17) Wei, T.; Carignano, M. A.; Szleifer, I. Lysozyme adsorption on polyethylene surfaces: why are long simulations needed? *Langmuir* **2011**, *27* (19), 12074−12081.
(18) Satulovsky, J.; Carignano, M.; Szleifer, I. Kinetic and thermodynamic control of protein adsorption. *Proc. Natl. Acad. Sci. U. S. A.* **2000**, *97* (16), 9037−9041.
(19) Rechendorff, K.; Hovgaard, M. B.; Foss, M.; Zhdanov, V. P.; Besenbacher, F. Enhancement of protein adsorption induced by surface roughness. *Langmuir* **2006**, *22* (26), 10885−10888.
(20) Sajib, M. S. J.; Wei, Y.; Mishra, A.; Zhang, L.; Nomura, K.-i.; Kalia, R. K.; Vashishta, P.; Nakano, A.; Murad, S.; Wei, T. Atomistic Simulations of Biofouling and Molecular Transfer of Crosslinked Aromatic Polyamide Membrane for Desalination. *Langmuir* **2020**, *36* (26), 7658−7668.
(21) Jiang, W. H.; Wang, G. J.; He, Y. N.; Wang, X. G.; An, Y. L.; Song, Y. L.; Jiang, L. Photo-switched wettability on an electrostatic self-assembly azobenzene monolayer. *Chem. Commun.* **2005**, *28*, 3550−3552.
(22) Wei, T.; Carignano, M. A.; Szleifer, I. Molecular Dynamics Simulation of Lysozyme Adsorption/Desorption on Hydrophobic Surfaces. *J. Phys. Chem. B* **2012**, *116* (34), 10189−10194.
(23) Zhang, T.; Wei, T.; Han, Y.; Ma, H.; Samieegohar, M.; Chen, P.-W.; Lian, I.; Lo, Y.-H. Protein−ligand interaction detection with a novel method of transient induced molecular electronic spectroscopy (TIMES): experimental and theoretical studies. *ACS Cent. Sci.* **2016**, *2* (11), 834−842.
(24) Wei, T.; Ma, H.; Nakano, A. Decaheme cytochrome MtrF adsorption and electron transfer on gold surface. *J. Phys. Chem. Lett.* **2016**, *7* (5), 929−936.
(25) Wei, T.; Sajib, M. S. J.; Samieegohar, M.; Ma, H.; Shing, K. Self-Assembled Monolayers of an Azobenzene Derivative on Silica and Their Interactions with Lysozyme. *Langmuir* **2015**, *31* (50), 13543−13552.
(26) Nakano, C. M.; Ma, H.; Wei, T. Study of lysozyme mobility and binding free energy during adsorption on a graphene surface. *Appl. Phys. Lett.* **2015**, *106* (15), 153701.
(27) Zheng, J.; Li, L.; Tsao, H.-K.; Sheng, Y.-J.; Chen, S.; Jiang, S. Strong repulsive forces between protein and oligo (ethylene glycol) self-assembled monolayers: a molecular simulation study. *Biophys. J.* **2005**, *89* (1), 158−166.
(28) Raffaini, G.; Ganazzoli, F. Molecular dynamics simulation of the adsorption of a fibronectin module on a graphite surface. *Langmuir* **2004**, *20* (8), 3371−3378.
(29) Penna, M. J.; Mijajlovic, M.; Biggs, M. J. Molecular-level understanding of protein adsorption at the interface between water and a strongly interacting uncharged solid surface. *J. Am. Chem. Soc.* **2014**, *136* (14), 5323−5331.
(30) Wei, T.; Huang, T.; Qiao, B.; Zhang, M.; Ma, H.; Zhang, L. Structures, dynamics, and water permeation free energy across bilayers of lipid A and its analog studied with molecular dynamics simulation. *J. Phys. Chem. B* **2014**, *118* (46), 13202−13209.
(31) Wei, T.; Zhang, L.; Zhao, H.; Ma, H.; Sajib, M. S. J.; Jiang, H.; Murad, S. Aromatic polyamide reverse-osmosis membrane: an atomistic molecular dynamics simulation. *J. Phys. Chem. B* **2016**, *120* (39), 10311−10318.
(32) Van Der Munnik, N. P.; Sajib, M. S. J.; Moss, M. A.; Wei, T.; Uline, M. J. Determining the potential of mean force for amyloid-β dimerization: combining self-consistent field theory with molecular dynamics simulation. *J. Chem. Theory Comput.* **2018**, *14* (5), 2696−2704.
(33) Shaw, D. E.; Maragakis, P.; Lindorff-Larsen, K.; Piana, S.; Dror, R. O.; Eastwood, M. P.; Bank, J. A.; Jumper, J. M.; Salmon, J. K.; Shan, Y.; Wriggers, W. Atomic-level characterization of the structural dynamics of proteins. *Science* **2010**, *330* (6002), 341−346.
(34) Voth, G. A. *Coarse-Graining of Condensed Phase and Biomolecular Systems.*; CRC Press: Boca Raton, FL, 2008.
(35) Jahan Sajib, M. S.; Sarker, P.; Wei, Y.; Tao, X.; Wei, T. Protein Corona on Gold Nanoparticles Studied with Coarse-Grained Simulations. *Langmuir* **2020**, *36* (44), 13356−13363.
(36) Marrink, S. J.; Risselada, H. J.; Yefimov, S.; Tieleman, D. P.; De Vries, A. H. The MARTINI force field: coarse grained model for biomolecular simulations. *J. Phys. Chem. B* **2007**, *111* (27), 7812−7824.
(37) Alder, B. J.; Wainwright, T. E. Studies in Molecular Dynamics. I. General Method. *J. Chem. Phys.* **1959**, *31* (2), 459−466.
(38) Rapaport, D. C. Molecular dynamics simulation of polymer chains with excluded volume. *J. Phys. A: Math. Gen.* **1978**, *11* (8), L213−L217.
(39) Rapaport, D. C. Molecular dynamics study of a polymer chain in solution. *J. Chem. Phys.* **1979**, *71* (8), 3299−3303.
(40) Rapaport, D. The event scheduling problem in molecular dynamic simulation. *J. Comput. Phys.* **1980**, *34* (2), 184−201.
(41) Zhou, Y.; Karplus, M. Folding thermodynamics of a model three-helix-bundle protein. *Proc. Natl. Acad. Sci. U. S. A.* **1997**, *94* (26), 14429−32.
(42) Dokholyan, N. V.; Buldyrev, S. V.; Stanley, H. E.; Shakhnovich, E. I. Discrete molecular dynamics studies of the folding of a protein-like model. *Folding Des.* **1998**, *3* (6), 577−87.
(43) Voegler Smith, A.; Hall, C. K. alpha-helix formation: discontinuous molecular dynamics on an intermediate-resolution protein model. *Proteins: Struct., Funct., Genet.* **2001**, *44* (3), 344−360.
(44) Ding, F.; Dokholyan, N. V.; Buldyrev, S. V.; Stanley, H. E.; Shakhnovich, E. I. Molecular dynamics simulation of the SH3 domain aggregation suggests a generic amyloidogenesis mechanism. *J. Mol. Biol.* **2002**, *324* (4), 851−7.
(45) Ding, F.; Borreguero, J. M.; Buldyrey, S. V.; Stanley, H. E.; Dokholyan, N. V. Mechanism for the alpha-helix to beta-hairpin transition. *Proteins: Struct., Funct., Genet.* **2003**, *53* (2), 220−228.
(46) Javidpour, L.; Tabar, M. R.; Sahimi, M. Molecular simulation of protein dynamics in nanopores. I. Stability and folding. *J. Chem. Phys.* **2008**, *128* (11), 115105.

https://dx.doi.org/10.1021/acs.jctc.0c01172
J. Chem. Theory Comput. 2021, 17, 1874−1882

(47) Javidpour, L.; Tabar, M. R.; Sahimi, M. Molecular simulation of protein dynamics in nanopores. II. Diffusion. *J. Chem. Phys.* **2009**, *130* (8), 085105.
(48) Wagoner, V. A.; Cheon, M.; Chang, I.; Hall, C. K. Computer simulation study of amyloid fibril formation by palindromic sequences in prion peptides. *Proteins: Struct., Funct., Genet.* **2011**, *79* (7), 2132−2145.
(49) Javidpour, L.; Sahimi, M. Confinement in nanopores can destabilize alpha-helix folding proteins and stabilize the beta structures. *J. Chem. Phys.* **2011**, *135* (12), 125101.
(50) Hernandez de la Pena, L.; van Zon, R.; Schofield, J.; Opps, S. B. Discontinuous molecular dynamics for rigid bodies: applications. *J. Chem. Phys.* **2007**, *126* (7), 074106.
(51) Ding, F.; Tsao, D.; Nie, H.; Dokholyan, N. V. Ab initio folding of proteins with all-atom discrete molecular dynamics. *Structure* **2008**, *16* (7), 1010−8.
(52) Shirvanyants, D.; Ding, F.; Tsao, D.; Ramachandran, S.; Dokholyan, N. V. Discrete molecular dynamics: an efficient and versatile simulation method for fine protein characterization. *J. Phys. Chem. B* **2012**, *116* (29), 8375−82.
(53) Yanez Orozco, I. S.; Mindlin, F. A.; Ma, J.; Wang, B.; Levesque, B.; Spencer, M.; Rezaei Adariani, S.; Hamilton, G.; Ding, F.; Bowen, M. E.; Sanabria, H. Identifying weak interdomain interactions that stabilize the supertertiary structure of the N-terminal tandem PDZ domains of PSD-95. *Nat. Commun.* **2018**, *9* (1), 3724.
(54) Zheng, S.; Javidpour, L.; Shing, K. S.; Sahimi, M. Dynamics of proteins aggregation. I. Universal scaling in unbounded media. *J. Chem. Phys.* **2016**, *145* (13), 134306−134313.
(55) Zheng, S.; Shing, K. S.; Sahimi, M. Dynamics of proteins aggregation. II. Dynamic scaling in confined media. *J. Chem. Phys.* **2018**, *148* (10), 104305−104314.
(56) Zheng, S.; Sahimi, A.; Shing, K. S.; Sahimi, M. Molecular dynamics study of structure, folding, and aggregation of poly-glycine-alanine (Poly-GA). *J. Chem. Phys.* **2019**, *150* (14), 144307−144312.
(57) Zheng, S.; Sahimi, A.; Shing, K. S.; Sahimi, M. Molecular Dynamics Study of Structure, Folding, and Aggregation of Poly-PR and Poly-GR Proteins. *Biophys. J.* **2021**, *120* (1), 64−72.
(58) Karanicolas, J.; Brooks, C. L., 3rd. The structural basis for biphasic kinetics in the folding of the WW domain from a formin-binding protein: lessons for protein design? *Proc. Natl. Acad. Sci. U. S. A.* **2003**, *100* (7), 3954−9.
(59) Karanicolas, J.; Brooks, C. L., 3rd. Integrating folding kinetics and protein function: biphasic kinetics and dual binding specificity in a WW domain. *Proc. Natl. Acad. Sci. U. S. A.* **2004**, *101* (10), 3432−7.
(60) Hills, R. D., Jr.; Brooks, C. L., 3rd. Insights from coarse-grained Go models for protein folding and dynamics. *Int. J. Mol. Sci.* **2009**, *10* (3), 889−905.
(61) Wei, S.; Knotts, T. A. t. A coarse grain model for protein-surface interactions. *J. Chem. Phys.* **2013**, *139* (9), 095102.
(62) Li, Y.; Wei, S.; Wu, J.; Jasensky, J.; Xi, C.; Li, H.; Xu, Y.; Wang, Q.; Marsh, E. N. G.; Brooks, C. L.; Chen, Z. Effects of Peptide Immobilization Sites on the Structure and Activity of Surface-Tethered Antimicrobial Peptides. *J. Phys. Chem. C* **2015**, *119* (13), 7146−7155.
(63) Wei, S.; Zou, X.; Cheng, K.; Jasensky, J.; Wang, Q.; Li, Y.; Hussal, C.; Lahann, J.; Brooks, C. L.; Chen, Z. Orientation Determination of a Hybrid Peptide Immobilized on CVD-Based Reactive Polymer Surfaces. *J. Phys. Chem. C* **2016**, *120* (34), 19078−19086.
(64) Wei, S.; Zou, X.; Tian, J.; Huang, H.; Guo, W.; Chen, Z. Control of Protein Conformation and Orientation on Graphene. *J. Am. Chem. Soc.* **2019**, *141* (51), 20335−20343.
(65) Zou, X.; Wei, S.; Badieyan, S.; Schroeder, M.; Jasensky, J.; Brooks, C. L., 3rd; Marsh, E. N. G.; Chen, Z. Investigating the Effect of Two-Point Surface Attachment on Enzyme Stability and Activity. *J. Am. Chem. Soc.* **2018**, *140* (48), 16560−16569.
(66) Zheng, S.; Javidpour, L.; Sahimi, M.; Shing, K. S.; Nakano, A. sDMD: An open source program for discontinuous molecular dynamics simulation of protein folding and aggregation. *Comput. Phys. Commun.* **2020**, *247*, 106873.
(67) Nguyen, H. D.; Hall, C. K. Kinetics of fibril formation by polyalanine peptides. *J. Biol. Chem.* **2005**, *280* (10), 9074−82.
(68) Marchut, A. J.; Hall, C. K. Effects of chain length on the aggregation of model polyglutamine peptides: molecular dynamics simulations. *Proteins: Struct., Funct., Genet.* **2007**, *66* (1), 96−109.
(69) Wang, Y.; Shao, Q.; Hall, C. K. N-terminal Prion Protein Peptides (PrP(120−144)) Form Parallel In-register beta-Sheets via Multiple Nucleation-dependent Pathways. *J. Biol. Chem.* **2016**, *291* (42), 22093−22105.
(70) Zou, X.; Wei, S.; Jasensky, J.; Xiao, M.; Wang, Q.; Brooks, C. L.; Chen, Z. Molecular Interactions between Graphene and Biological Molecules. *J. Am. Chem. Soc.* **2017**, *139* (5), 1928−1936.
(71) Abraham, M. J.; Murtola, T.; Schulz, R.; Páll, S.; Smith, J. C.; Hess, B.; Lindahl, E. GROMACS: High performance molecular simulations through multi-level parallelism from laptops to supercomputers. *SoftwareX* **2015**, *1*, 19−25.
(72) Rizzo, R. C.; Jorgensen, W. L. OPLS all-atom model for amines: resolution of the amine hydration problem. *J. Am. Chem. Soc.* **1999**, *121* (20), 4827−4836.
(73) Jorgensen, W. L.; Maxwell, D. S.; Tirado-Rives, J. Development and testing of the OPLS all-atom force field on conformational energetics and properties of organic liquids. *J. Am. Chem. Soc.* **1996**, *118* (45), 11225−11236.
(74) Xie, Q.; Alibakhshi, M. A.; Jiao, S.; Xu, Z.; Hempel, M.; Kong, J.; Park, H. G.; Duan, C. Fast water transport in graphene nanofluidic channels. *Nat. Nanotechnol.* **2018**, *13* (3), 238−245.
(75) Ebrahim-Habibi, M.-B.; Ghobeh, M.; Mahyari, F. A.; Rafii-Tabar, H.; Sasanpour, P. An investigation into non-covalent functionalization of a single-walled carbon nanotube and a graphene sheet with protein G: A combined experimental and molecular dynamics study. *Sci. Rep.* **2019**, *9* (1), 1−18.
(76) Gao, J.; Wang, L.; Kang, S.-g.; Zhao, L.; Ji, M.; Chen, C.; Zhao, Y.; Zhou, R.; Li, J. Size-dependent impact of CNTs on dynamic properties of calmodulin. *Nanoscale* **2014**, *6* (21), 12828−12837.
(77) Zhao, D.; Li, L.; He, D.; Zhou, J. Molecular dynamics simulations of conformation changes of HIV-1 regulatory protein on graphene. *Appl. Surf. Sci.* **2016**, *377*, 324−334.
(78) Sawai, M. V.; Waring, A. J.; Kearney, W. R.; McCray, P. B., Jr; Forsyth, W. R.; Lehrer, R. I.; Tack, B. F. Impact of single-residue mutations on the structure and function of ovispirin/novispirin antimicrobial peptides. *Protein Eng., Des. Sel.* **2002**, *15* (3), 225−232.
(79) Zou, X.; Wei, S.; Jasensky, J.; Xiao, M.; Wang, Q.; Brooks, C. L., III; Chen, Z. Molecular interactions between graphene and biological molecules. *J. Am. Chem. Soc.* **2017**, *139* (5), 1928−1936.
(80) Wei, Y.; Latour, R. A. Correlation between desorption force measured by atomic force microscopy and adsorption free energy measured by surface plasmon resonance spectroscopy for peptide-surface interactions. *Langmuir* **2010**, *26* (24), 18852−61.
(81) Sawai, M. V.; Waring, A. J.; Kearney, W. R.; McCray, P. B., Jr; Forsyth, W. R.; Lehrer, R. I.; Tack, B. F. Impact of single-residue mutations on the structure and function of ovispirin/novispirin antimicrobial peptides. *Protein Eng., Des. Sel.* **2002**, *15* (3), 225−232.
(82) Zheng, S.; Javidpour, L.; Shing, K. S.; Sahimi, M. Dynamics of proteins aggregation. I. Universal scaling in unbounded media. *J. Chem. Phys.* **2016**, *145* (13), 134306−134313.
(83) Callender, R. H.; Dyer, R. B.; Gilmanshin, R.; Woodruff, W. H. Fast events in protein folding: the time evolution of primary processes. *Annu. Rev. Phys. Chem.* **1998**, *49*, 173−202.
(84) Shao, Q.; Hall, C. K. Protein adsorption on nanoparticles: model development using computer simulation. *J. Phys.: Condens. Matter* **2016**, *28* (41), 414019.
(85) Yu, G.; Liu, J.; Zhou, J. Mesoscopic coarse-grained simulations of lysozyme adsorption. *J. Phys. Chem. B* **2014**, *118* (17), 4451−4460.

https://dx.doi.org/10.1021/acs.jctc.0c01172
J. Chem. Theory Comput. 2021, 17, 1874−1882